THE ASTROPHYSICAL JOURNAL, 387:347–356, 1992 March 1

THE WIND GEOMETRY OF THE WOLF-RAYET STAR HD 191765

R. E. SCHULTE-LADBECK,[1] K. H. NORDSIECK, M. TAYLOR, K. S. BJORKMAN,
A. M. MAGALHÃES,[2] AND M. J. WOLFF
Space Astronomy Laboratory, University of Wisconsin at Madison, 1150 University Avenue, Madison, WI 53706
Received 1991 June 10; accepted 1991 September 9

ABSTRACT

We present a time-dependent spectropolarimetric data set of the single WN6 star HD 191765 in the wavelength range 3159 Å $\leq \lambda \leq$ 7593 Å. At all epochs our observations display a large and strongly wavelength-dependent continuum polarization and reduced levels of polarization across the emission lines. The data imply a significant intrinsic continuum polarization which requires a general deviation of the electron distribution from spherical symmetry. This global shape is quite stable as a function of time; small fluctuations may arise from localized density/temperature changes. The line polarizations are consistent with an axisymmetric wind geometry and ionization stratification. The polarized line profile of the He II line at 4686 Å is redshifted and of a different shape than the flux line profile, due to electron scattering of line photons in the expanding envelope. The intrinsic continuum polarization rises into the ultraviolet and cannot be understood by electron scattering alone. We develop a qualitative model for polarization in a Wolf-Rayet atmosphere. We argue that the blueward rise of the continuum polarization in HD 191765 can be explained if the density in the wind is high, resulting in a competition of thermal and electron-scattering continuum opacity in the optical. EZ CMa, on the other hand, displays a flat polarization spectrum at most epochs; we find that electron scattering is the main continuum opacity source at optical wavelengths.

Subject headings: polarization — stars: individual (HD 191765) — stars: mass loss — stars: Wolf-Rayet

1. INTRODUCTION

Wolf-Rayet (W-R) stars are generally believed to be the descendants of massive and luminous OB stars which have lost most of their hydrogen-rich layers in a strong stellar wind. These winds may be so thick that even the continua of W-R stars are formed in the extended atmospheres. Basic stellar parameters such as effective temperature and gravity are not easily defined because W-R stars have no single radius or position at which the optical depth at all frequencies is of order unity. Only through models can we infer the stellar properties.

Recent advances in the modeling of stellar atmospheres have led to the development of a "standard model" for W-R stars (Hamann, Schmutz, & Wessolowski 1988; Hillier 1987a, b, 1988). The prerequisites of the standard-model atmosphere are spherical geometry, a monotonic velocity law, homogeneity, and stationary time-dependence. The model provides a good match to the observed continua of W-R stars and to the strengths of He I and He II lines, and it also predicts a stratified ionization structure. However, it gives incorrect metal strengths, P Cygni absorptions on some lines that are too deep, and electron-scattering line wings which are too strong (see Hillier 1991).

We are here concerned with observational tests of the assumptions and consequences of the standard model. The method that we employ is time-dependent, optical, linear spectropolarimetry. In this way we use as a tool the property that these stars are engulfed in dense, electron-scattering envelopes. A net polarization is observed only when the extended atmosphere is not spherical or homogeneous. Polarization of a W-R star provides a measure of the product of the geometry of the scattering volume, its orientation, and electron-scattering optical depth. If the column density of free electrons varies in the W-R wind, e.g., due to a variable mass-loss rate or changes in the ionization state of the wind material, it may introduce a time-variable continuum polarization even for a single star. An important diagnostic of spectropolarimetry is the polarization across emission lines. When the polarization varies at the line wavelengths, we refer to the "line effect" being observed in this star. The optical lines in W-R stars are produced by unpolarized recombination emission. Although they might be polarized by subsequent electron scattering, we assume that we can use the polarizations at line center to eliminate the foreground polarization introduced by the interstellar medium on the line of sight to the star by extrapolating to a minimal line polarization. If some lines still display polarization after interstellar polarization removal, we can infer that the electron-scattering optical depth in the envelope is significant to these lines and study the ionization stratification. It is also expected that the macroscopic velocity field of the electrons imprints itself on the profile of the emission lines (Auer & van Blerkom 1972; Hillier 1984); such electron-scattering wings should be polarized in a nonspherical wind geometry.

We have developed and applied tools to interpret spectropolarimetric data of W-R stars in two papers (Schulte-Ladbeck et al. 1990, Paper I; and Schulte-Ladbeck et al. 1991, Paper II). Both concerned the WN 5 star EZ CMa (=HD 50896 = WR 6). We discussed the possible effects that line and continuum opacities, in addition to the geometry, may have on the observed polarization, and put forward a model of an inclined, rotating, and expanding disk for the inner wind in EZ CMa. The word "disk" is used as an illustrative term, describing a prevailing polarization and thus aspherical density distribution. Mass loss into all directions from the stellar surface is expected for luminous stars because the basic driving mechanism, the radiation, exerts its force in all directions. However,

[1] Now at Department of Physics and Astronomy, University of Pittsburgh, Pittsburgh, PA 15260.
[2] On leave from Instituto Astronômico e Geofísico, Universidade de São Paulo, Brazil.

contrary to OB stars, the W-R stars display the famous "momentum problem," meaning that the momentum in the flow exceeds significantly the one in the radiation field. For EZ CMa, we have speculated that rotation might be important for the envelope geometry; if true, it may enhance the driving and also may have influenced the structure of the stellar interior. Also, if multiple scattering is effective (and with a suitable distribution of driving lines), the momentum problem will become less severe.

Although EZ CMa has been chosen as the WN-prototype of the standard model, it is potentially a dubious case because of the alleged presence of a compact companion (Firmani et al. 1980). HD 191765, once put in that same category, has recently been rehabilitated as a single star (Moffat & Robert 1991). The interpretation of our data will thus be less ambiguous.

HD 191765 is an already well-known example for local wind asymmetries. It has been suggested to have a disk-shaped wind geometry by Underhill et al. (1990) on the basis of line-profile analyses. The wind is not homogeneous as a function of time according to Robert, Moffat, & Seggewiss (1991), who interpreted the proliferation of small emission humps in the line profiles by outwardly propagating "blobs" of material. The linear polarization in a wide filter was measured by Robert et al. (1989) and found indicative of a preferred symmetry axis in the system. Schmidt (1988) presented a spectropolarimetric data set of HD 191765 and suggested that the aspherical geometry of the continuum is shared by the emission lines.

We first investigate HD 191765 and then compare the results with EZ CMa which is the only other case for which time-dependent spectropolarimetric data are available. HD 191765 and EZ CMa are both WNE-B stars, early WN stars with strong lines. We note that these two stars are located very close to one another in the Hertzsprung-Russell diagram constructed from the standard model (Hamann 1991). Accordingly, they are both hot and have high mass-loss rates, and hydrogen is virtually absent, implying that they are fairly advanced in their evolution.

2. RESULTS

The data were obtained during the second half of 1990 with the medium-resolution, high-throughput, dual-beam spectropolarimeter on the 0.9 m telescope at the Pine Bluff Observatory of the University of Wisconsin. A detailed description of the instrument and our calibration procedures was given in Paper II. We measured the three Stokes parameters Q, U, and I simultaneously over the spectral range from 3159 to 7593 Å. The seven nights of spectropolarimetry were co-added to increase the signal-to-noise ratio in the polarization, and a "triplot" (a plot of the relative flux, percentage polarization, and equatorial position angle as a function of wavelength) of the combined spectrum is shown in Figure 1.

A journal of observations is given in Table 1, where we list the polarization integrated over the spectral range for comparison with filter data. The polarizations and position angles of our data are in good agreement with the B filter observations published by Robert et al. (1989), also in variability amplitude and direction. As can be seen from Figure 1, the spectrum of HD 191765 is crowded with lines. The polarization changes markedly in the emission lines. In order to investigate the temporal variability and the slope of the continuum polarization, we have defined seven "line-free" continuum filters. The wavelength windows that we used are from 3561 to 3669 Å, 4413 to 4449 Å, 5001 to 5139 Å, 5565 to 5703 Å, 5955 to 6021 Å, 6777 to 6855 Å, and 7257 to 7485 Å. (Subsequent line-polarization measurements were corrected using these continuum bands.) In Table 1, we then also give the line-free continuum polarization as a function of time. A plot of these data is presented in Figure 2. Two results are apparent from Figure 2. The line-free continuum polarization is larger, by on average ~0.15%, because the lines act as depolarizers. Second, the position angle of the time series appears to be different. With the wide-filter polarimetry, one might suggest from the localized band of polarizations in the Q-U plane, a preferred direction of the stellar variability at a position angle of ~24° on the sky; however, with the continuum-only data, this axis may be instead at an orientation of ~61°. The amplitude of continuum variability is 0.19% in Q and 0.21% in U, or four times the typical 1 σ error of 0.05% in each Stokes parameter (using the χ^2 test, we found that the probability that it could be constant is ~3.5% for Q and slightly over 1% for U). Compare this to the variability in the strongest emission line, He II λ4686,

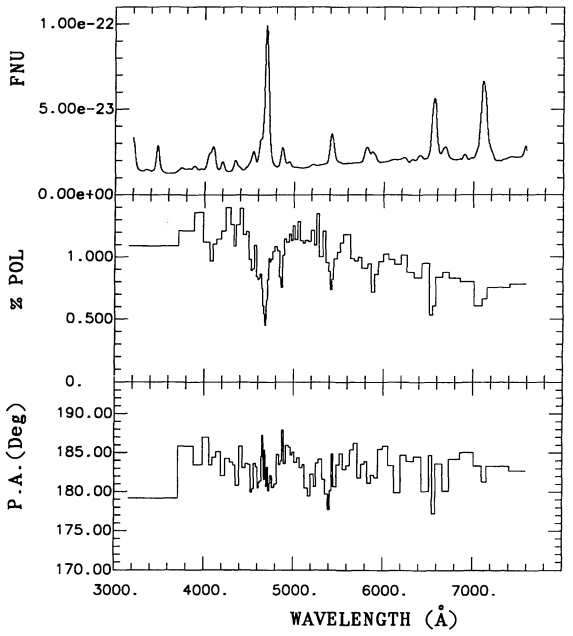

FIG. 1.—The spectropolarimetric data obtained during seven nights in 1990 were co-added to create this higher signal-to-noise, time-averaged data set of HD 191765. The flux in ergs cm^{-2} s^{-1} Hz^{-1}, degree of linear polarization in %, and equatorial position angle in degrees are plotted as a function of wavelength in Å. The polarimetric data were binned to an error of 0.07% polarization. The percentage polarization is strongly wavelength-dependent; it drops significantly in the emission lines and displays a smooth decline in the continuum. The position angle appears to be constant as a function of wavelength.

TABLE 1

ALL SPECTRUM AND CONTINUUM-ONLY DATA

1990 Date	Q_{ALL} (%)	U_{ALL} (%)	σ_{ALL} (%)	Q_{CONT} (%)	U_{CONT} (%)	σ_{CONT} (%)
Jun 24	0.93	0.01	0.01	1.18	0.03	0.04
Aug 24	0.86	0.06	0.02	0.99	0.10	0.05
Sep 03	0.99	0.12	0.01	1.09	0.17	0.04
Oct 22	0.95	0.11	0.01	1.13	0.17	0.04
Nov 01	0.95	0.11	0.02	1.11	0.09	0.05
Dec 01	0.99	0.17	0.02	1.02	0.19	0.05
Dec 02	0.98	0.08	0.02	1.03	0.24	0.05

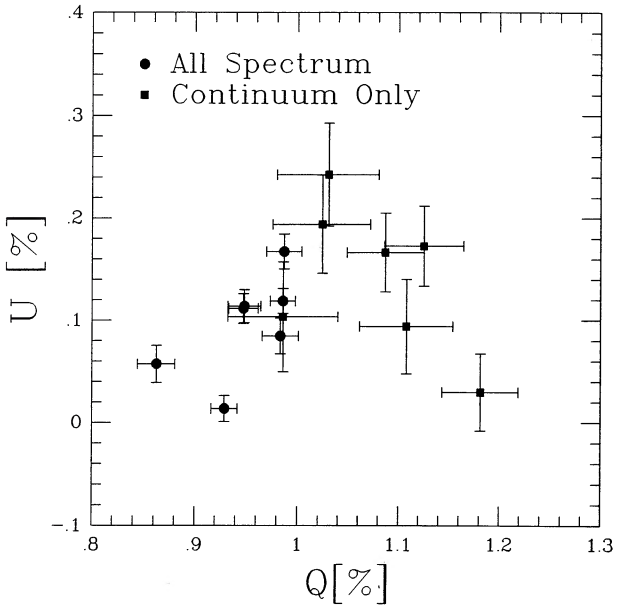

FIG. 2.—*Q-U* diagram showing the polarization data integrated over the whole spectrum, and the line-free continuum-only polarization for the seven nights of observation. The continuum polarization is larger than the all-spectrum polarization because the emission lines are less polarized than the continuum.

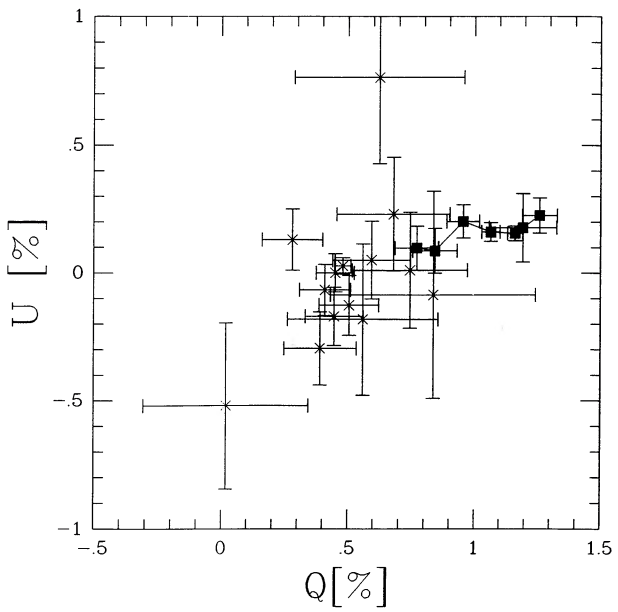

FIG. 4.—*Q-U* diagram of line polarizations (x) and line-free continuum polarizations (filled squares). The continuum polarizations are connected to show their systematic spectral behavior; the point farthest out is the bluest one, the polarization decreases toward the red, at a constant position angle. The line polarizations form a band of data points with the same position angle and extending to even smaller polarizations. This indicates that some lines are intrinsically polarized in the same direction as the continuum, as expected in a stratified, axisymmetric envelope.

of amplitudes 0.46% in Q and 0.25% in U with a typical error of 0.08% (see also Fig. 3). The χ^2 test reveals that the probability that it could be constant is 0.1% for Q and 53% for U. We may conclude that the polarization displays significant variability in the continuum and the He II λ4686 emission line. We note that the equivalent width of the line is variable, too.

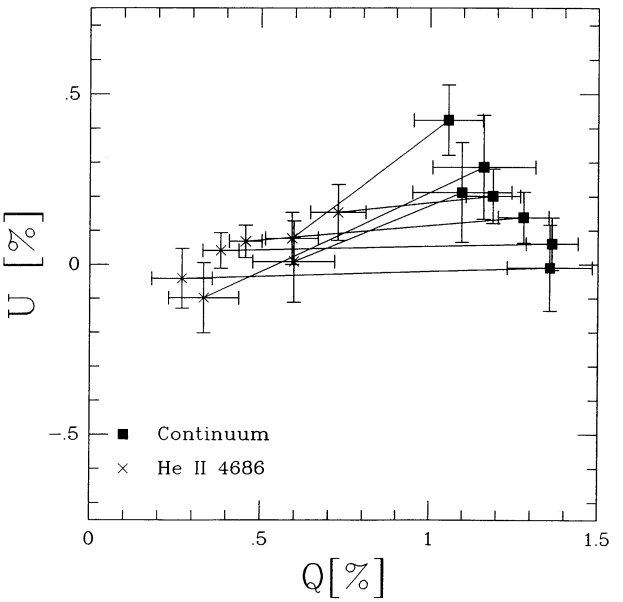

FIG. 3.—*Q-U* diagram of He II 4686 line polarizations (x) and 4686-continuum polarizations (filled squares). Measurements taken from the same spectrum are connected to show the continuum-to-line color vectors. If the line were totally unpolarized, a continuum polarization of greater than 1% would be indicated. The line and continuum polarization vary as a function of time.

We investigated the wavelength dependence of the continuum in the *Q-U* plane as a function of time. At all epochs, the bluest spectral data are located farthest away from the zero-point of the *Q-U* diagram, and a path to smaller polarizations is traced with increasing wavelength, consistent with a constant position angle. (The mean continuum wavelength path can be seen in Fig. 4.) The continuum has a color dependence at all times. This color dependence is different from the one expected if the polarization were chiefly due to interstellar foreground polarization, which peaks usually at intermediate optical wavelengths, and specifically at $\sim$5600 Å for R_V, the ratio of total-to-selective extinction, equal to 3.1, i.e., a "normal" sightline. Large interstellar polarization consequently produces a curly wavelength track because of this maximum. We note that in EZ CMa we observed a cluster of wavelength-independent data points at most epochs, which we interpreted as the superposition of a Thomson-scattering continuum with a small interstellar vector.

The wavelength dependence of the continuum data in HD 191765 is intriguing. Superposition of the interstellar and intrinsic polarization vectors is expected to cause a rotation of the observed position angle with wavelength because the two generally have different position angles and wavelength dependencies. The constancy of the position-angle spectrum of HD 191765 implies that the interstellar polarization is either negligible, or that it fortuitously points either in the same direction as the stellar continuum polarization, or at 90° (=180° in the *Q-U* plane) away from it. The former angle amounts to subtraction, and the latter to addition, of intrinsic continuum polarization.

As for EZ CMa, we attempted to estimate the interstellar foreground polarization by using the assumption that the

TABLE 2

OBSERVED POLARIZATIONS IN COMBINED DATA

Filter (Å)	Q (%)	U (%)	σ (%)
3561–3669	1.19	0.18	0.13
4413–4449	1.26	0.23	0.07
5001–5139	1.16	0.16	0.03
5565–5703	1.06	0.16	0.04
5955–6021	0.95	0.20	0.07
6777–6855	0.84	0.09	0.09
7257–7485	0.77	0.10	0.09
He I 5876	0.02	−0.52	0.33
He II 4100	0.59	0.05	0.15
He II 4200	0.84	−0.09	0.41
He II 4339	0.56	−0.18	0.30
He II 4542	0.39	−0.30	0.14
He II 4859	0.28	0.13	0.12
He II 5411	0.41	−0.07	0.10
He II 6560	0.45	−0.17	0.11
He II 4686	0.48	0.03	0.03
N IV 4058	0.68	0.23	0.22
N IV 7117	0.50	−0.13	0.12
N V 4945	0.62	0.76	0.34
N V + N III	0.45	0.00	0.08
C IV + N IV	0.74	0.01	0.23

emission lines should, to first order, be unpolarized. We defined 30 Å wide filters centered on the flux peaks of the lines. We carried out two types of measurements. First, for the very strong He II line at 4686 Å, we measured the polarization in the line and the underlying continuum for each individual night. The data are displayed in Figure 3. The data show that both the observed continuum and line polarization are variable. We use the continuum-to-line color vectors to find the convergence point which then represents an upper limit on the interstellar polarization, at a wavelength of 4686 Å. The values thus obtained are $\sim -0.1\%$ in U and 0.15% in Q. An important result emerges. If we shift the origin of the Q-U diagram to this new value (meaning that we are taking out the interstellar vector at 4686 Å), the remaining polarization in the continuum is still appreciable, namely over 1%. Such a large value of the continuum polarization requires a pronounced aspherical density distribution of the scattering electrons or a continuum source that is in itself not spherical.

Second, we measured the polarizations in the other emission lines visible in Figure 1, the combined data. The results are given in Table 2. The line and continuum polarizations are displayed in Figure 4. We observe a narrow band of line polarizations, extending from the continuum toward smaller Q-U values. The emission lines of HD 191765 are less polarized than the continuum but in the same direction. If all lines were intrinsically unpolarized (and because the interstellar polarization is not expected to vary much as a function of wavelengths over the small spectral range covered by our observations), their polarizations should be similar. Since this is not the case the lines must be intrinsically polarized by different amounts, a first indication of stratification. This band of line-polarization data is identical, to within the errors, to Schmidt's (1988) observations (see his Fig. 4). We conclude that the overall envelope geometry in the radial direction and its orientation/symmetry do not change with time. A good model for the constant position angles as a function of radius is an axisymmetric wind. The smaller the observed line polarizations, the closer they are to the interstellar component. We used both Schmidt's and our sets of data to extrapolate to another upper limit on the interstellar polarization. The values are $U = -0.15\%$ and $Q = 0.10\%$, close to our first estimate from the minimum of the He II 4686 line polarizations.

Because the interstellar polarization comes out to be so small from the lines, i.e., $P = 0.18\%$ at $\Theta = 118°$, it does not make much difference to the intrinsic continuum slope where we place $\lambda_{\max}$. R_V is not constrained, and the lower limit on E_{B-V} implied by the amount of interstellar polarization is very small, 0.02.

Robert et al. (1989) published a map of the polarization in the region around HD 191765. They used for an estimate of the interstellar polarization 43 stars of known polarization, within a 2° radius of HD 191765 on the sky and a distance-modulus range of ± 2.5 mag centered at 11.2 mag. According to Robert et al., the interstellar polarization is $P = 1.176\% \pm 0.166\%$ and $\Theta = 144.^{\circ}4 \pm 7.^{\circ}7$. This value is very different from the one indicated by the line polarizations. However, the field-star method is generally not very reliable, because the parameters of the field stars, derived from catalog data, are less well known than those of the program star, and because the polarization does not simply become larger with distance like the reddening. If, for instance, the line of sight to the object passes through more than one interstellar cloud with different orientations of the magnetic field, the polarization of a more distant object may actually be smaller than the polarization of a closer one. As we are looking into the Cygnus spiral arm toward HD 191765, it may be expected that the light passes through multiple clouds. Indeed, inspecting the sky chart of Robert et al., one notices that the position angles vary by 90° in the vicinity of HD 191765.

We show that applying the field-star data to determine the interstellar polarization appropriate to HD 191765 leads to implausible results. Using a $\lambda_{\max}$ of 5600 Å for both estimates, line (interstellar model A) and field-star (interstellar model B) method, we calculated the interstellar polarization, subtracted it from the observed data, and plotted the results in Figure 5 in comparison to the uncorrected data. Model A results in an increase in the intrinsic continuum polarization; the slope of the continuum remains, as well as the dips at the line wavelengths. The dispersion of the position angles as a function of wavelength decreases slightly. With model B, on the other hand, the slope of the continuum polarization becomes much smaller, and the line dips are much less; this would make an attractive pure electron-scattering continuum. However, now the position angle has developed a pronounced wavelength dependence, and all the lines stick out, an unlikely result because it requires at least two intrinsic scattering planes for the continuum and different scattering angles yet for the lines.

A wavelength and time-averaged continuum-only intrinsic polarization of 1.22% results after correction with model A. Such a large continuum polarization compares only to the polarizations observed from the highly flattened envelopes of Be stars. We measured the individual continuum-filter and line polarizations again in the corrected spectrum. To separate the polarization in the line, Q_L, from the observed polarization at the line wavelength, Q_T, we used the expression derived in equation (21) of Paper II, where Q_C is the continuum polarization and I_L/I_C is the line-to-continuum flux ratio

$$Q_L = Q_C[(Q_T/Q_C)(1 + I_L/I_C) - 1]/(I_L/I_C) ,$$

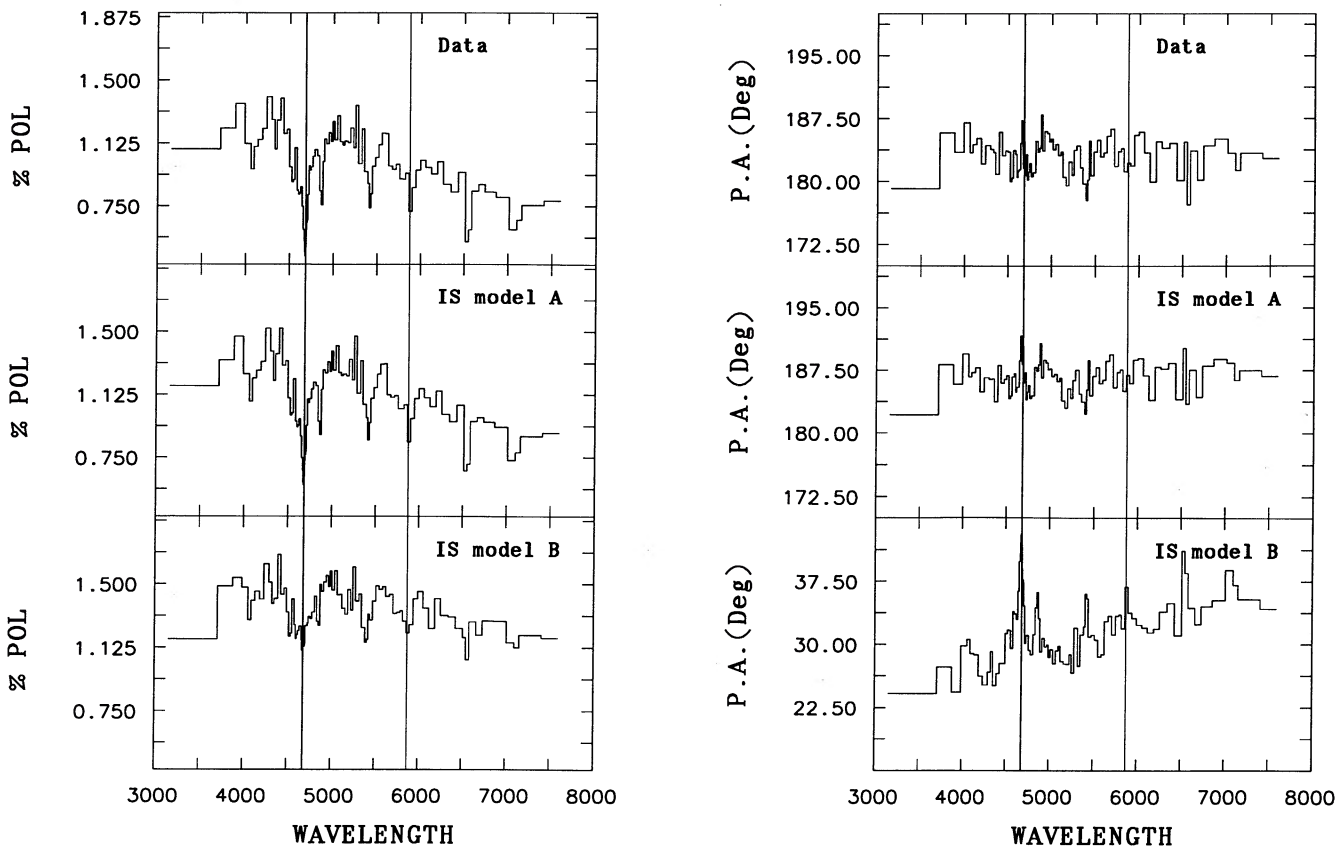

FIG. 5.—Comparison of percentage-polarization (*left*) and position-angle (*right*) spectra of the data as observed (*top panels*), and after being corrected with two different models for the interstellar polarization, all binned to 0.07%. IS model A (*middle*) assumes the minimum value consistent with the emission-line polarizations; IS model B (*bottom*) is based on the field-star method. The positions of the He II 4686 and the He I 5876 lines are marked, to help the eye in comparing line features. One can see that the assumed interstellar-polarization correction, A or B, has a profound influence on the "intrinsic" polarization spectrum; the interpretation hinges on the quality of the IS model.

and the same for U. This formula defines our observable quantity which we call line polarization. For optically thin emission lines it has a simple physical interpretation, i.e., it is the polarization of the line photons. In the optically thick case the line can destroy continuum photons, and hence the polarized intensities are not additive (see eq. [19] of Paper II). In Hillier's model of EZ CMa, He II λ4686, for example, is an optically thick line. We then divided the Q and U parameters of the lines by their underlying continuum polarizations; the results are shown in Figure 6. A similar normalization was used in Paper II for EZ CMa, except that we divided by the Q and U parameters of the continuum. Then the continuum polarization assumes a value of 1, an unpolarized line has a value of 0, and lines with intermediate polarizations but position angles that are the same as the continuum's fall along a 45° line. Effectively, this normalization gave up the information about the true position angles on the plane of the sky. The new normalization used for Figure 6 now has the continuum on a circle with radius 1, an unpolarized line at the center of the circle, and partially polarized lines anywhere in between, depending on their position angles.

In Figure 6, we use different symbols to highlight lines with different ionization potentials (IPs), e.g., the He I line at 5876 Å, the He II line at 4686 Å, and the N V line at 4945 Å. The ionization stratification in the wind is apparent, with lines of higher IP originating from closer to the star. This was first

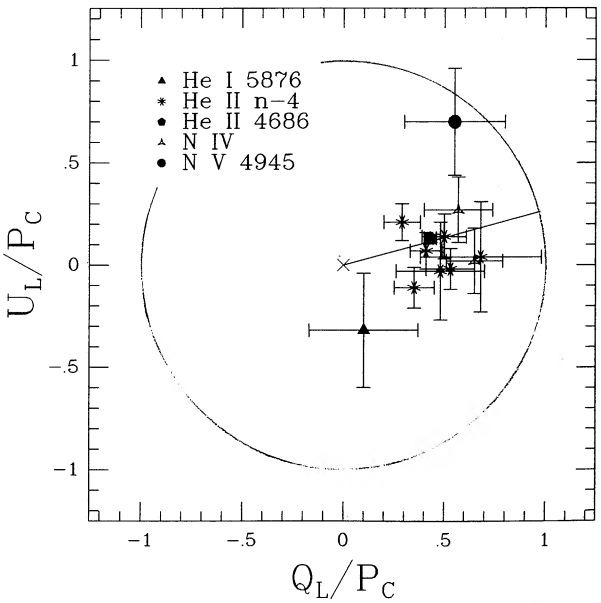

FIG. 6.—Diagnostic diagram for atmospheric stratification. In this normalization, the continuum polarization is 1, and an unpolarized emission line has a polarization of 0. The line represents fractional polarizations at the same position angle as the continuum polarization. Different symbols were used for different lines.

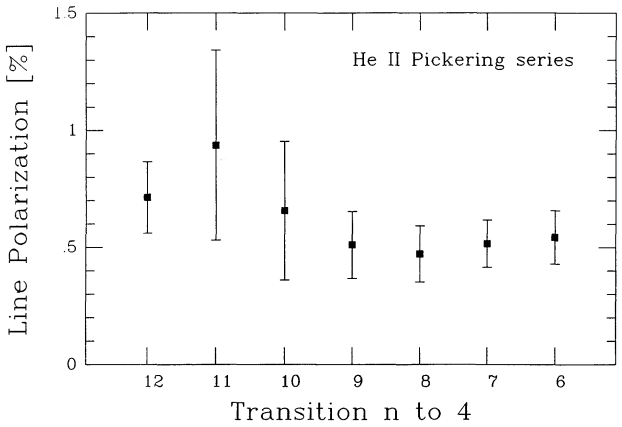

FIG. 7.—The He II Pickering series polarizations as a function of transition upper level. Almost all of these lines are blended with lines that may have different polarizations, the 12–4 (4100 Å), 10–4 (4339 Å), and 9–4 (4542 Å) transitions are probably the most afflicted ones. A constant would describe the data, as would a curve of increasing polarization toward higher levels, which is the expected form.

TABLE 3

INTRINSIC POLARIZATION ACROSS THE He II 4686 LINE

Bin (Å)	Q (%)	U (%)	σ (%)	P (%)	Θ (°)
4437–4455.....	1.243	0.273	0.101	1.273	6.20
4581–4593.....	0.932	0.285	0.092	0.975	8.51
4647–4659.....	0.785	0.303	0.056	0.841	10.55
4659–4665.....	0.647	0.280	0.064	0.705	11.69
4665–4671.....	0.637	0.223	0.055	0.675	9.66
4671–4677.....	0.577	0.171	0.052	0.601	8.26
4677–4683.....	0.544	0.229	0.064	0.591	11.43
4683–4689.....	0.597	0.228	0.055	0.639	10.46
4689–4695.....	0.708	0.181	0.055	0.730	7.17
4695–4701.....	0.752	0.161	0.057	0.769	6.02
4701–4707.....	0.767	0.171	0.069	0.786	6.29
4707–4719.....	0.913	0.236	0.066	0.943	7.23
4719–4731.....	1.091	0.151	0.067	1.101	3.93
4731–4743.....	1.063	0.182	0.065	1.078	4.87
4743–4755.....	1.086	0.221	0.073	1.108	5.74
4755–4779.....	1.103	0.186	0.072	1.119	4.79
4779–4797.....	1.169	0.089	0.076	1.172	2.19
4797–4809.....	1.249	0.297	0.114	1.284	6.69

pointed out by Schmidt. His plot of observed line polarization versus IP gave the correct result because the interstellar polarization is so small. In comparison with the EZ CMa stratification, we note that the He II 4686 line is again highly polarized. According to the model by Hillier (1987b) in which He II 4686 forms at comparatively low electron densities, one might expect this line to be less polarized than that which is observed. The N V line in HD 191765, as well as the N IV 4058 line in EZ CMa, show quite different position angles than the continua. In EZ CMa, the He II Pickering lines had surprisingly low polarizations; in HD 191765 they appear to adopt higher values, between He II 4686 and N IV, as expected from the EZ CMa–model electron densities. Schmidt indicated a possible trend of changing polarization along the He II Pickering series. In Figure 7, we display the He II line polarization as a function of transition upper level. A constant would describe the data, as would a curve of increasing polarization toward higher levels, which is the expected form. (Note that the 12–4 transition at 4100 Å, the 10–4 at 4339 Å, and 9–4 at 4542 Å suffer from severe blending with other lines.) Clearly, more data are needed to investigate this issue.

We discovered a Q-U loop as a function of wavelength across the strong line of He II 4686 in the time-averaged data of EZ CMa and attributed it to the combined effect of rotation and expansion of a flattened and inclined atmosphere (Paper I). We ask whether such a loop is apparent also in HD 191765. Because of the blends in the blue wing of the line, we selected a continuum band on the blue side between 4437 and 4455 Å. We also used a region between the He II 4542 line and the N V + N III blend at 4640 Å, between 4581 and 4593 Å, then picked up the whole profile longward of the blend out to the red continuum and terminated it at 4809 Å. The results were slightly binned; the data are given in Table 3 and displayed in Figure 8. The total drop in polarization is large, ~0.7% in HD 191765, compared to only ~0.3% in EZ CMa. With an average width of the structure of ~0.15%, it is narrower than that observed in EZ CMa (~0.2%). The large axis ratio, 0.7/0.15, contributes in making a loop harder to detect in HD 191765 than in EZ CMa (0.3/0.2). The 1 σ errors are larger, too, typically 0.06% in HD 191765 compared to 0.03% in EZ CMa.

Two features are conspicuous. The blue wing of the profile displays systematically higher U values than the red wing, i.e., if the true feature were a simple drop to a minumum value, the large errors might be expected to cause a "crossing-over" of the data points and not a systematic blue-red split, and second, the minimum of the polarization does not coincide with the flux line peak. The latter asymmetry was also observed in EZ CMa. We therefore believe that the loop in HD 191765 is real. The sense of rotation is opposite to that of EZ CMa; if related

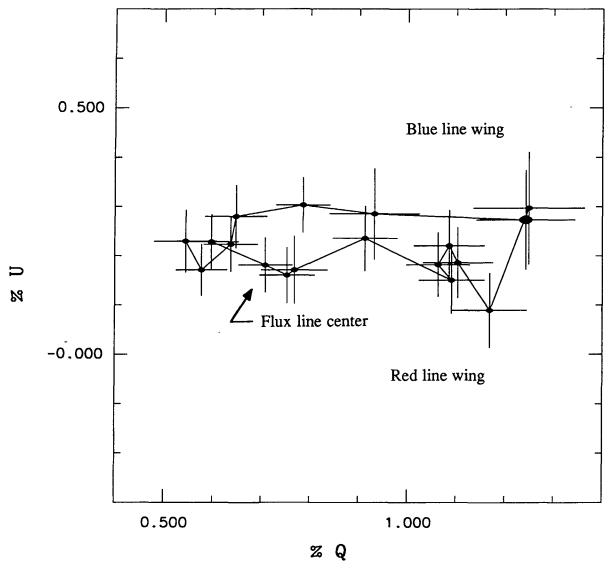

FIG. 8.—The polarization across the He II 4686 line in the Q-U plane. The large data point is the bluest one, a continuum filter. The second data point, connected to the first one, is a filter located between the He II 4542 and the N V + N III 4640 lines and is already within the blue wing of the profile. The data points continue contiguously through the line profile and into the continuum on the red side of the line. An asymmetry of the minimum polarization with respect to the flux line peak is apparent. There is a systematic behavior of the blue-and red-wing polarizations, indication that this structure is a loop traced counterclockwise. The depth of the feature is ~0.7%, its width is ~0.15%, the error bars are ~ ±0.06%.

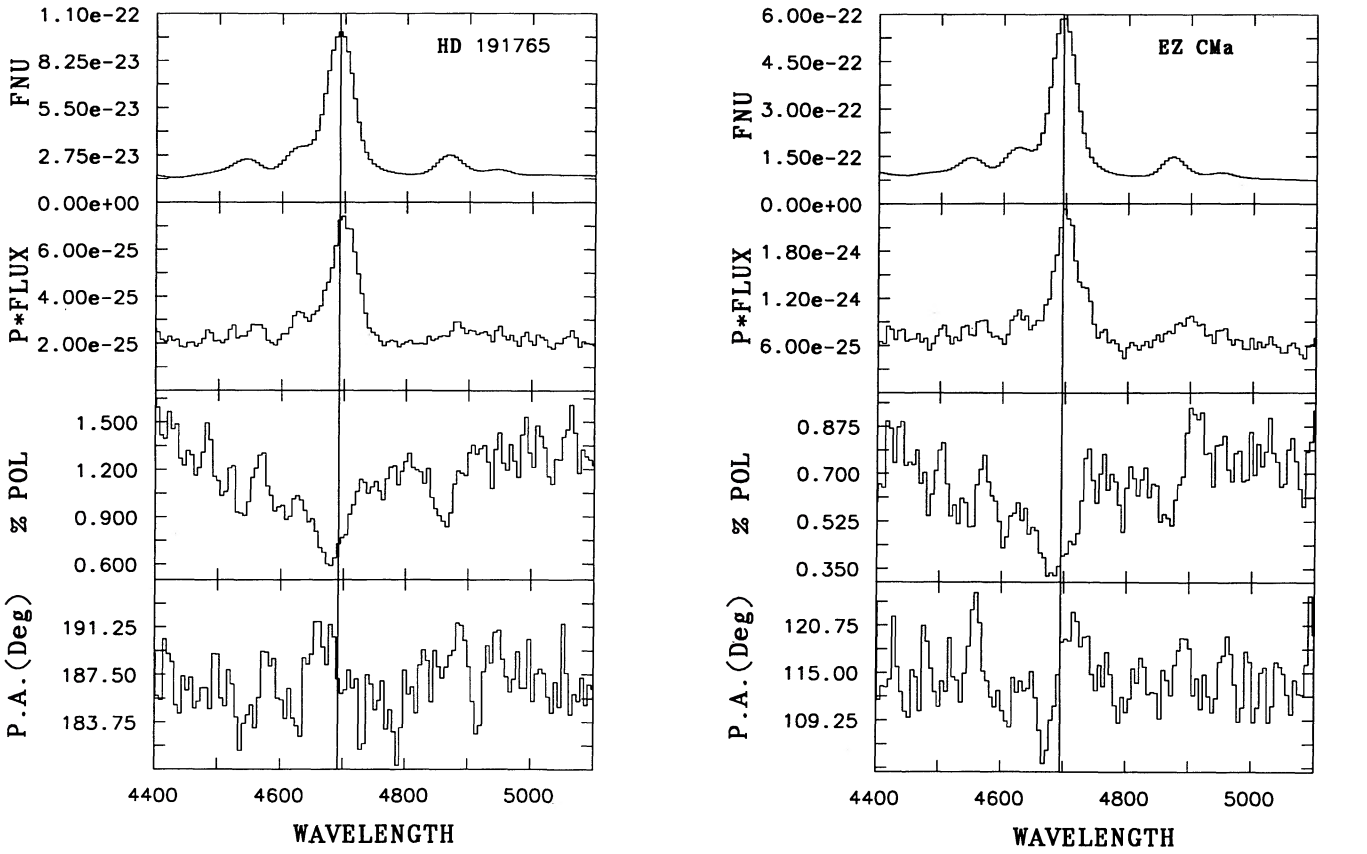

FIG. 9.—A comparison of the flux, polarized flux, percentage polarization, and position angle spectra of HD 191765 (*left*) and EZ CMa (*right*) in the wavelength region from 4400 to 5100 Å. All data are unbinned. A vertical line was drawn in each one at the observed position of the flux peak of the He II 4686 line. The polarized-flux profiles display steep blue wings (resolving the N V + N III blend better in polarized flux than in flux), and redshifted polarized-flux peaks. They are quite similar in both stars. In EZ CMa the red wing is extremely extended. In both stars, the minimum of percentage polarization occurs on the blue side of the flux-line center. In EZ CMa the position angle rotation across the line is apparent even in the unbinned data.

to stellar rotation, this just means that HD 191765 spins counterclockwise.

For another comparison of the polarization across He II 4686, we plot in Figure 9 the flux, polarized flux, percentage polarization, and position angle for both HD 191765 and EZ CMa in the region from 4400 to 5100 Å. The 4686 line profiles of both stars are very different in polarized flux than in flux. The polarized line peaks are redshifted, the red line wings are extended compared to the flux profiles, and the blue wings of the polarized line profiles are much steeper than the flux profiles. In both stars, the minima of percentage polarizations occur on the blue side of the flux peaks. In EZ CMa, one can distinguish the position angle rotation that ultimately causes the *Q-U* loop. (Note that we display unbinned observations in this figure.) Thus, we potentially observe three processes in the polarized He II line profile. First, there is extra polarized emission on the red wings. Second, there is either absorption or missing emission of polarized radiation on the blue wings. Third, there is a separation of the blue and red wing polarizations in position angles.

From Figure 3 it became apparent that the amount of polarization of the He II 4686 line also varies as a function of time, while the position angle of the variation coincides with the overall orientation of the atmosphere. No simple relation emerges, e.g., with the equivalent width of the line, or the continuum polarization. The same was true for EZ CMa.

3. DISCUSSION

Any model of the Wolf-Rayet stars HD 191765 and EZ CMa will have to account for the following observations.

1. The light from both stars displays intrinsic linear polarization at optical wavelengths.

2. The continuum polarization of EZ CMa is constant as a function of wavelength in all but one of our data sets. The continuum polarization of HD 191765 decreases as a function of wavelength in all observations, from $\sim$1.5% at 4000 Å to 0.7% at 7000 Å in our co-added spectrum.

3. The polarization of both objects shows the line effect, i.e., a decrease in polarization at the wavelengths of emission lines.

4. In both stars, there is still some polarization even at line center for N V 4945 and He II 4686, while there is close to none in He I 5876.

5. The polarization and polarized flux across He II 4686 show an asymmetry with respect to the flux line center in both objects.

6. The polarization across He II 4686 displays a loop in the *Q-U* plane in both stars.

7. The polarization varies as a function of time in both stars, in both the continuum and the He II 4686 line (which is our highest signal-to-noise line observation).

We wish to restate which of these conclusions are sensitive to the interstellar polarization correction. The results on the line effect, presence of intrinsic polarization and partial polar-

izations in lines which are different for different lines, as well as variability, and the shape of the He II 4686 Q-U loop are independent of the adopted interstellar polarization. The exact shape of the continuum polarization spectrum depends on the interstellar polarization correction; however, as we have shown in Paper II for EZ CMa and above for HD 191765, for reasonable values of P_{max} and λ_{max} (and thus R_V), the slope of the EZ CMa spectrum is flat (at all but one epoch), whereas that of HD 191765 rises into the UV. The line polarizations themselves were derived after correction for interstellar polarization, and thus our quantitative results depend on it. The shapes of the polarized flux profiles of He II 4686 are very sensitive to the adopted interstellar correction.

In Paper I we discussed the Q-U loop across He II 4686. The systematic position-angle changes from the blue to the red line wing indicate that the spatial integration over the envelope "seen" by photons in the blue wing of the line is systematically different from that seen by photons in the red wing of the line. We argued that such a spatial/velocity separation could be accounted for in an envelope that is expanding and rotating and which we do not view exactly edge-on.

We also noticed a "shoulder" on the red polarized-flux wing of He II 4686 in EZ CMa. A redshifted polarized-flux line profile with a steep blue wing and a strong red wing is again observed in HD 191765. We previously attributed the presence of line polarization to Thomson scattering by free electrons in the wind. We neglected the aspect that the scattering electrons are not at rest. In expanding envelopes, the ions and electrons are moving away from one another, so that each ion "sees" the wind material expanding away from it. The situation is similar to the Hubble flow of galaxies. While the process of electron scattering is independent of frequency in the electron's rest frame, the expansion causes a redistribution of line photons in the star's rest frame. On the red wing, polarized photons emerge which have been scattered from the high-flux line center and shifted to the red, causing the appearance of a strong red polarized line wing. In the blue line wing most of the polarized flux is that scattered from shorter wavelengths where the flux in the profile is small. The redshift by electron scattering explains both the steep blue wing and the percentage polarization minimum on the blue side of line center. In addition, photons originally emitted on the blue side of line center are more likely to suffer absorption by ions when the line is optically thick, since they are scattered toward the line center in wavelength. Note that while electron-scattering wings have been detected in the flux profiles (see Hillier 1984), the effect is more easily seen in polarized flux because it shows the spectrum of the scattered radiation only.

We propose that these polarized-flux profiles present a new diagnostic (for a given geometry) of envelope expansion, i.e., the velocity law, through their redshift, for the wind temperature structure through their widths, and the electron density profile through the polarized-flux line strengths. We note that Underhill & Yang (1991) observed increasing mean radial velocities in several He II lines of EZ CMa toward lines with lower upper levels along the Pickering series. This is compatible with the model of Hillier (1987b) in which the Pickering lines are formed at increasing mean radii and in the accelerating part of the velocity law, and our interpretation of these redshifts as being caused by electron scattering.

The presence of intrinsic polarization demands deviations from spherical symmetry in the star or envelope. In Paper II, we proposed that an axisymmetric wind is responsible for the polarization of EZ CMa. However, possibly this envelope structure is caused by tidal forces exerted by a neutron-star companion on an originally spherically symmetric wind and not by an intrinsic axisymmetry of the W-R star. For the single star HD 191765 the position-angle constancy of the continuum and the line polarizations again provide strong evidence that the wind geometry is axisymmetric. In this object, such a geometry finds a natural explanation in stellar rotation.

In Paper II we also discussed polarization variability. Such changes reflect temporal variations in the optical depth of the free electron scatterers. The variations may be caused by either density or temperature changes in the wind, or changes in the geometry. We attributed these variations to clumpiness which could be caused by self-initiating wind perturbations in the flow as modeled by Owocki (1991) for O and B stars. Alternatively, they could be related to variability in the star itself (e.g., pulsations). In addition to global asymmetries of the winds, our data are thus indicative of local inhomogeneities as well, with variability time scales as short as the minimum separation of the observations, i.e., 1 day.

In EZ CMa, the continuum polarization is constant as a function of wavelength for all but one data set, in which it displayed a rise of polarization toward shorter wavelengths. We argued in Paper II that this new wavelength behavior might have been caused by a dense clump in which the optical depth of thermal processes (i.e., bound-free and free-free absorption) which increases with wavelength between absorption edges was competing with the wavelength-independent electron-scattering optical depth. In HD 191765 we are also faced with a continuum polarization that rises to shorter wavelengths in the optical spectral range; however, this occurs at all times of observation.

Schmidt (1988) was puzzled by this spectral shape of the polarization HD 191765. He observed a smooth decline of the polarization from a value of $\sim$1.4% at 4200 Å to $\sim$0.9% at 8200 Å. To reduce the level of polarization by this much toward longer wavelengths through dilution by unpolarized emission requires that the unpolarized component contribute nearly 40% of the light there. A similar, 50%, contribution in the red is implied by our data (corrected for interstellar polarization). A competing unpolarized absorptive opacity would have the same effect on the polarization spectrum; in particular, this could produce large changes in the polarization spectrum that are unaccompanied by large flux-spectrum features. Schmidt argued that according to Hillier, Jones, & Hyland (1983) one expects bound-free emission to dominate over free-free emission in the optical for reasonable temperatures. If optically thin bound-free emission/absorption were acting on the polarization, one then should see polarization jumps corresponding to He recombination edges. The data, both Schmidt's and ours, do not display polarization discontinuities. As a source which smoothly increases in relative importance to the red, Schmidt then suggested free-free emission from the wind. This would require a significant tail of optically thin emission extending into the optical. The actual contribution of optically thin free-free emission to the spectra of W-R stars is a model-dependent quantity; to determine it is beyond the scope of this paper.

Models for polarization by electron scattering have been developed for the case of optically thin, pure electron scattering, and optically thin electron scattering plus optically thin absorption and emission in a hydrogen envelope (see McLean 1979). For an observer in the equatorial plane of an oblate

envelope, the angle of polarization is perpendicular to the equatorial plane. The amount of polarization is proportional to the electron-scattering optical depth (as long as $\tau_{es} < 1$) and so is independent of wavelength. Both absorption and unpolarized reemission of light in the envelope can modify the wavelength-dependence, because of the frequency dependency in the opacities, causing polarization changes in the emission lines, across bound-free discontinuities, and in the continua. Optically thick pure electron scattering, also called multiple scattering, was modeled for an ellipsoidal geometry using a Monte Carlo approach (Daniel 1980), but the effects of thermal absorption and reemission were not included.

In order to explain the wavelength-dependence of the polarization of both EZ CMa and HD 191765, we present a qualitative model in which electron-scattering and thermal opacities are both important. The situation is illustrated in Figure 10. The model is based on the fact that polarization is suppressed by multiple scatterings. All processes which take place at depths below an optical depth of almost unity in either electron scattering or thermal absorption emerge from the stellar wind as almost unpolarized. Almost all of the polarization must be introduced by the last scattering by the electrons, which by definition occurs above the $\tau_{es} = 1$ depth. In the extended atmospheres of W-R stars, the radius at which the average photon of a given wavelength is created from thermal emission processes, i.e., the thermalization depth, is in general, different from the radius at which the photon is last scattered. When electron scattering is the dominant contributor to the opacity at a given wavelength, the radius of the star may be defined to be the distance at which $\tau_{es} \approx 1$, while a different stellar radius is defined by the condition $\tau_{th} = 1$ for wavelengths at which the thermal bound-free and free-free opacities dominate electron scattering. Because the thermal opacities increase with wavelength, the radius of a star with an extended atmosphere is larger in the infrared than in the UV.

In Figure 10, we exemplify this atmospheric extension and the effects that a wavelength-dependent radius may have on the polarization. For short-wavelength radiation created inside of the radius where $\tau_{es} \approx 1$, the photons are multiple-scattered before they emerge. The polarized intensity reaches a maximum near where $\tau_{es} \approx 1$ integrated from this radius of "last scattering" out to infinity. (Some polarized radiation may be destroyed on its way out through the wind, because even a $\tau_{es} < 1$ does not mean a zero chance for scattering.) The polarization is almost constant as a function of wavelength for all radiation created with $\tau_{th}(\nu) < \tau_{es} \approx 1$ because the polarization is introduced by scattering from the same electrons at all wavelengths. There will be a decrease of the polarization with wavelength because of the emission of unpolarized photons by thermal processes in the regions where $\tau_{es} \leq 1$.

As the monochromatic thermal optical depth increases with wavelength, the radius of the thermalization depth will eventually become larger than the electron-scattering radius. The electron-scattering optical depth from these radii out to infinity consequently decreases and the continuum polarization drops toward longer wavelengths because of the growing size of the unpolarized thermal emission volume ("continuum stratification"). The turnover in the slope of the polarization spectrum may thus yield information on the stellar radius. In the same way we can interpret the decrease of polarization in the lines because the lines form at larger radii than the continuum, as well as the different amounts of line polarizations because of the ionization stratification in the envelope. Additional factors contributing to the decrease of the continuum polarization with wavelength are free-free absorption and the depolarization which results from the less-forward-peaked radiation field seen by the scattering electrons as the atmospheric extension grows.

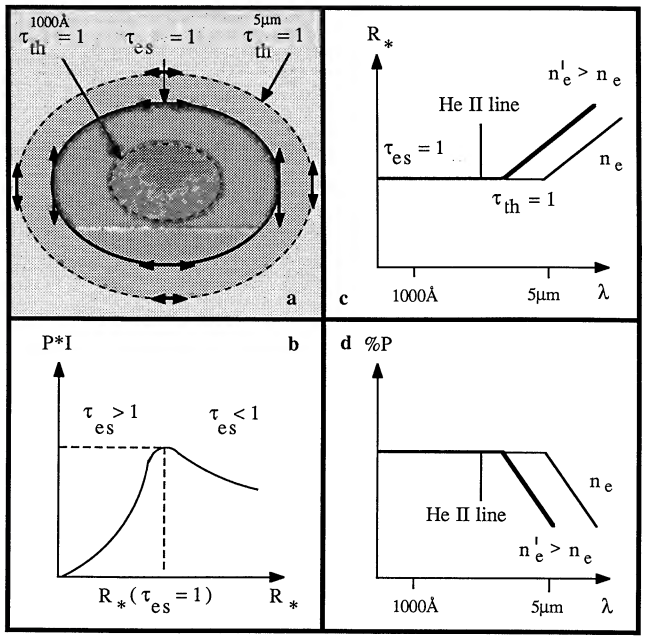

FIG. 10.—Optically thick wind model. The density distribution is assumed to be of axisymmetric (ellipsoidal) geometry, and the observer is located in the equatorial plane. (*a*) In an extended atmosphere, the radius of creation, $\tau_{th}(\nu) = 1$, at a given frequency is different from the radius of last scattering, $\tau_{es} = 1$. For all photons with $\tau_{th}(\nu) < \tau_{es} \approx 1$ (e.g., at 1000 Å), the radius of the star is the same namely the radius of last scattering; at long wavelengths (e.g., 5 μm) the photons are created outside of the $\tau_{es} = 1$ layer. (*b*) Inside of the $\tau_{es} = 1$ radius, multiple scattering destroys the polarization. The maximum polarization is reached at $\tau_{es} \approx 1$. The observer sees a polarized star. (*c*) The radius of the star is a function of wavelength. Emission lines (e.g., of He II) are always formed at larger radii than the continuum. (*d*) The larger the formation radius, the smaller the electron-scattering optical depth from that radius out to infinity, and the smaller is the polarization (continuum and lines). Note the prediction of a turnover in the polarization spectrum depending on wind density (n_e or n'_e).

We can now address why the continuum polarization spectra of EZ CMa and HD 191765 have different slopes while originating from the same physical processes. The basic physical reason is that the electron-scattering opacity is proportional to n_e, while the thermal emission is proportional to n_e^2. We suggest that the electron-scattering opacity completely dominates in the optical waveband in EZ CMa because of its lower wind density as compared to HD 191765 and that the optical continuum photons in EZ CMa are created by thermal processes below the base of the wind. We conclude that the envelope is very extended. In HD 191765, we observe a competition of the electron scattering with the thermal emission at optical wavelengths creating a rapid decrease of the polarization as a function of wavelength. We are led to the conclusion that the atmosphere of HD 191765 is less extended. This can be understood by a steeper density gradient; the radius of creation starts to grow outside of the radius of the last scattering at optical frequencies.

Our interpretation of the polarization data is in agreement with the empirical models of Schmutz, Hamann, & Wessol-

owski (1989) for the two stars under scrutiny. Their observations indicate very similar terminal velocities, and their models yield the same mass-loss rates, for both stars. However, the radii (and thus temperatures and luminosities) differ. For EZ CMa, the radius at the base of the wind is 5 $R_\odot$, the corresponding radius for HD 191765 is 3.5 $R_\odot$. The radius where the Rosseland optical depth equals $\frac{2}{3}$ is at 18 $R_\odot$ for EZ CMa, while it occurs at 14 $R_\odot$ for HD 191765. The equation of continuity thus implies a steeper density gradient and higher densities in the atmosphere of HD 191765 as compared to EZ CMa.

4. PREDICTIONS

The interpretation of our observations encourages us to make the following predictions that can be tested by future observations and modeling:

1. The polarization of EZ CMa should decrease rapidly in the IR, beyond the wavelength at which the electron-scattering and thermal opacities are almost equal. According to Hillier et al. (1983), the optical depth at 2 μm is unity where the electron-scattering depth is unity; we thus predict that the polarization spectrum turns over at 2 μm and drops steadily to longer wavelengths.

2. The polarization of HD 191765 should display a turnover to a flatter spectral slope at short enough wavelengths in the UV because at sufficiently small wavelengths the thermalization depth will always be much below the layer where $\tau_{es} \approx 1$.

3. According to the standard model, the atmospheric extension of WNE-B types is the largest of all W-R stars. Our interpretation implies that polarization wavelength-dependence should occur in other W-R stars of this particular subtype, provided that the wind geometries are not spherical. Alternatively, a nonspherical geometry might be the trademark of WNE-B stars; this, too, can be tested observationally.

4. It may be possible to arrive at a better match of observed and model line profiles when the deviations from spherical geometry (globally and locally) and rotation in addition to the electron scattering of line photons in an expanding envelope are being included. It remains to be seen how unique such many-parameter solutions can be; certainly there is a large number of lines for which we can gather flux and polarized-flux profiles.

5. The electron-scattered radiation field is significant in EZ CMa and HD 191765. Together with rotation it should aid in developing hydrodynamic wind models with smaller momentum problems.

Operating Pine Bluff Observatory is a team effort. We thank the dedicated observers for collecting and Marilyn R. Meade and Brian L. Babler for reducing the data. R. S.-L. gratefully acknowledges many interesting discussions with Drs. Arthur D. Code and John S. Mathis on extended atmospheres, and the suggestions made by the referee, Dr. D. J. Hillier. We made use of the SIMBAD database, operated at CDS, Strasbourg, France. This work was supported by NASA contract NAS5-26777 to the Wisconsin Ultraviolet Photo-Polarimeter-Experiment.

REFERENCES

Auer, L. C., & van Blerkom, D. 1972, ApJ, 178, 175
Daniel, J. Y. 1980, A&A, 86, 198
Firmani, C., Koenigsberger, G., Bisiacchi, G. F., Moffat, A. F. J., & Isserstedt, J. 1980, ApJ, 239, 607
Hamann, W.-R. 1991, in IAU Symposium 143, Wolf-Rayet Stars and Interrelations with Other Massive Stars in Galaxies, ed. K. A. van der Hucht & B. Hadayat, (Dordrecht: Kluwer), 81
Hamann, W.-R., Schmutz, W., & Wessolowski, U. 1988, A&A, 194, 190
Hillier, D. J. 1984, ApJ, 280, 744
———. 1987a, ApJS, 63, 947
———. 1987b, ApJS, 63, 965
———. 1988, ApJ, 327, 822
———. 1991, in IAU Symposium 143, Wolf-Rayet Stars and Interrelations with Other Massive Stars in Galaxies, ed. K. A. van der Hucht & B. Hadayat (Dordrecht: Kluwer), 59
Hillier, D. J., Jones, T. J., & Hyland, A. R. 1983, ApJ, 271, 221
McLean, I. S. 1979, MNRAS, 186, 265
Moffat, A. F. J., & Robert, C. 1991, in IAU Symposium 143, Wolf-Rayet Stars and Interrelations with other Massive Stars in Galaxies, ed. K. A. van der Hucht & B. Hadayat, (Dordrecht: Kluwer), 109
Owocki, S. P. 1991, in IAU Symposium 143, Wolf-Rayet Stars and Interrelations with Other Massive Stars in Galaxies, ed. K. A. van der Hucht & B. Hadayat, (Dordrecht: Kluwer), 155
Robert, C., Moffat, A. F. J., & Seggewiss, W. 1991, in IAU Symposium 143, Wolf-Rayet Stars and Interrelations with Other Massive Stars in Galaxies, ed. K. A. van der Hucht & B. Hadayat, (Dordrecht: Kluwer), 147
Robert, C., Moffat A. F. J., Bastien, P. Drissen, L., & St.-Louis, N. 1989, ApJ, 347, 1034
Schmidt, G. D. 1988, in Polarized Radiation of Circumstellar Origin, ed. G. V. Coyne, S. J., A. M. Magalhães, A. F. J. Moffat, R. E. Schulte-Ladbeck, S. Tapia, & D. T. Wickramasinghe, (Vatican Observatory: University of Arizona Press), p. 641
Schmutz, W., Hamann, W.-R., & Wessolowski, U. 1989, A&A, 210, 236
Schulte-Ladbeck, R. E., Nordsieck, K. H., Nook, M. A., Magalhães, A. M., Taylor, M., Bjorkman, K. S., & Anderson, C. M. 1990, ApJ, 365, L19 (Paper I)
Schulte-Ladbeck, R. E., Nordsieck, K. H., Taylor, M., Nook, M. A., Bjorkman, K. S., Magalhães, A. M., & Anderson, C. M. 1991, ApJ, 382, 301 (Paper II)
Underhill, A. B., Gilroy, K. K., Hill, G. M., & Dinshaw, N. 1990, ApJ, 351, 666
Underhill, A. B., & Yang, S. 1991, ApJ, 368, 588